Electronic Supplementary Material (ESI) for Chemical Communications

Pseudorotaxanes from self-assembly of two crown ether-based cryptands and a 1,2-bis(pyridinium) ethane derivative

Xuzhou Yan,[a] Peifa Wei,[a] Binyuan Xia,[a] Feihe Huang*[a] and Qizhong Zhou*[b]

[a] *Department of Chemistry, Zhejiang University, 310027 Hangzhou, P. R. China.*

Fax and Tel: +86-571-8795-3189; Email address: fhuang@zju.edu.cn.

[b] *Department of Chemistry, Taizhou University, Taizhou 317000, P. R. China. E-mail: qizhongchou@tzc.edu.cn*

Electronic Supplementary Information (14 pages)

1. Materials and methods

All reagents were commercially available and used as supplied without further purification. Dibenzo-24-crown-8 (DB24C8, **1**) was obtained from Alfa Aesar and used as received. *cis*-DB24C8-based cryptand (**2**),[S1] bis(*m*-phenylene)-32-crown-10-based cryptand (**3**),[S2] and guest **4**[S3] were synthesized by published procedures. ^{1}H NMR spectra were recorded with a Bruker Advance DMX 400 spectrophotometer with use of the deuterated solvent as the lock and the residual solvent or TMS as the internal reference. Low-resolution electrospray ionization (LRESI) mass spectra were obtained on a Bruker Esquire 3000 plus mass spectrometer (Bruker-Franzen Analytik GmbH Bremen, Germany) equipped with ESI interface and ion trap analyzer. UV-vis spectroscopy was performed on a Shimadzu UV-2550 instrument at room temperature. The crystals data were collected on an Oxford Diffraction Xcalibur Atlas Gemini ultra. The crystal structure was solved by SHELXS-97[S4] and refined by SHELXL-97.[S5]

2. Job plots of ***2***$\supset$***4****, and* $\mathbf{3}_2\supset\mathbf{4}$ *based on UV-Vis spectroscopy data in acetone*

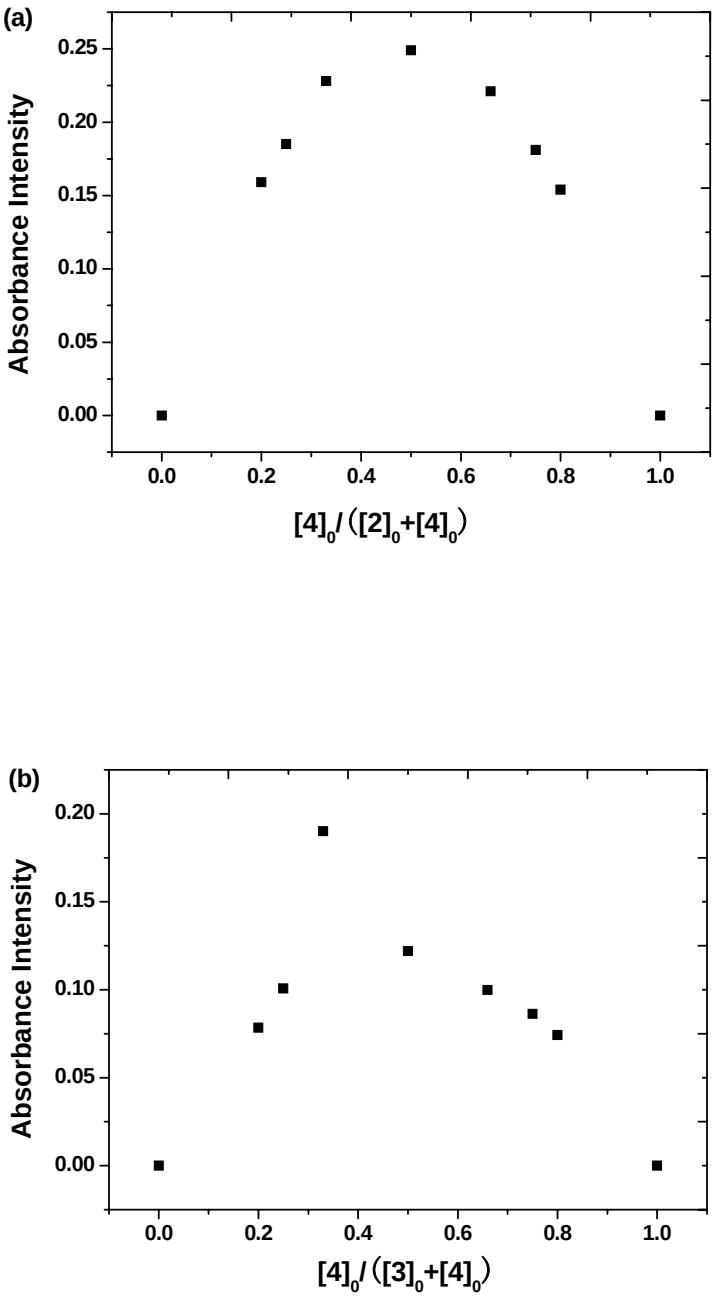

Fig. S1. Job plots showing the 1:1 stoichiometriy of the complex between **2** and **4** (a) and the 2:1 stoichiometry of the complex between **3** and **4** (b) in acetone: (a) $[\mathbf{2}]_0 + [\mathbf{4}]_0 = 2.00$ mM; (b) $[\mathbf{3}]_0 + [\mathbf{4}]_0 = 2.00$ mM. $[\mathbf{2}]_0$, $[\mathbf{3}]_0$, and $[\mathbf{4}]_0$ are the initial concentrations of **2**, **3** and **4**, respectively.

3. Electrospray ionization mass spectra of ***2*** *and* ***3*** *with guest* ***4*** *in acetone*

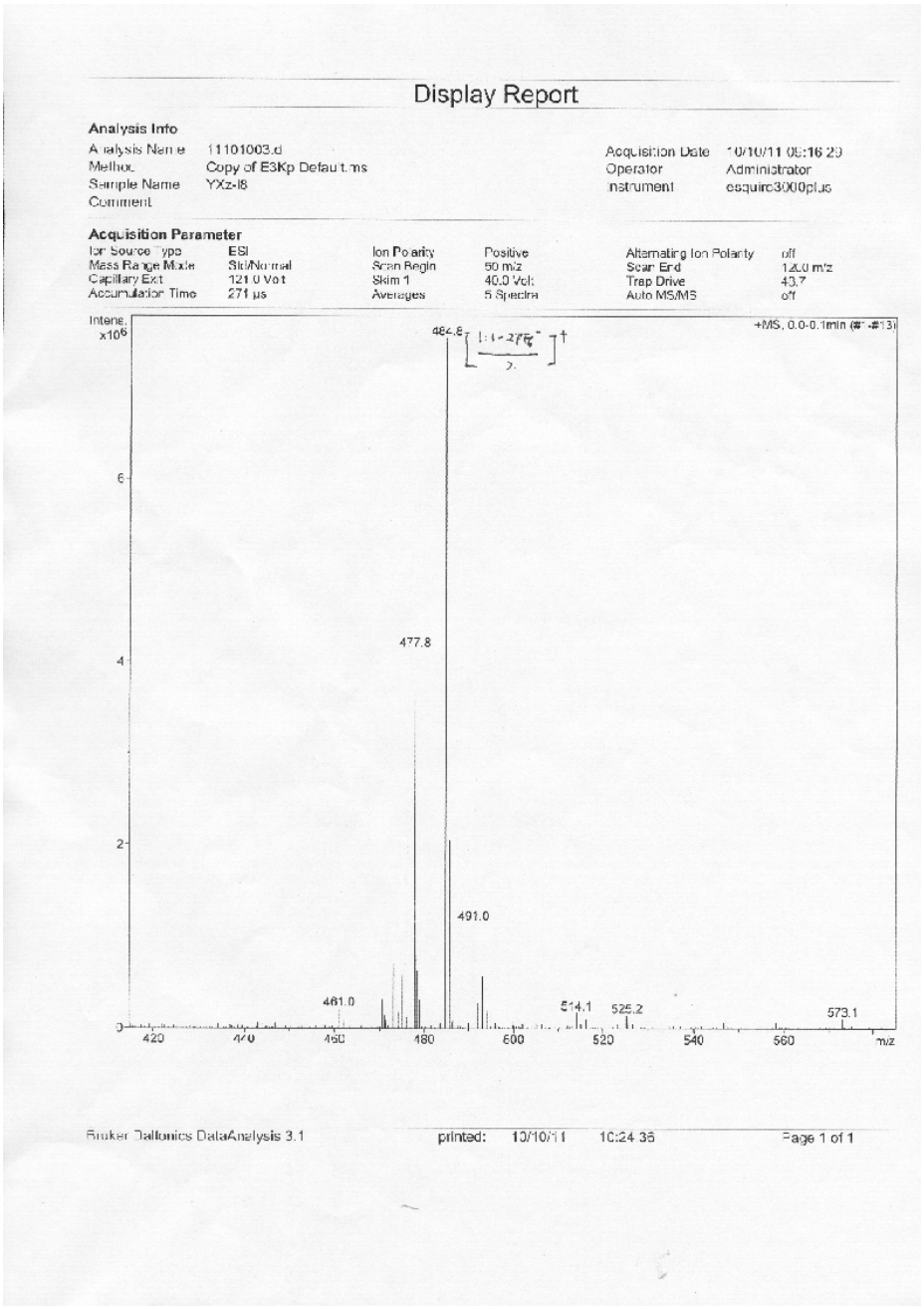

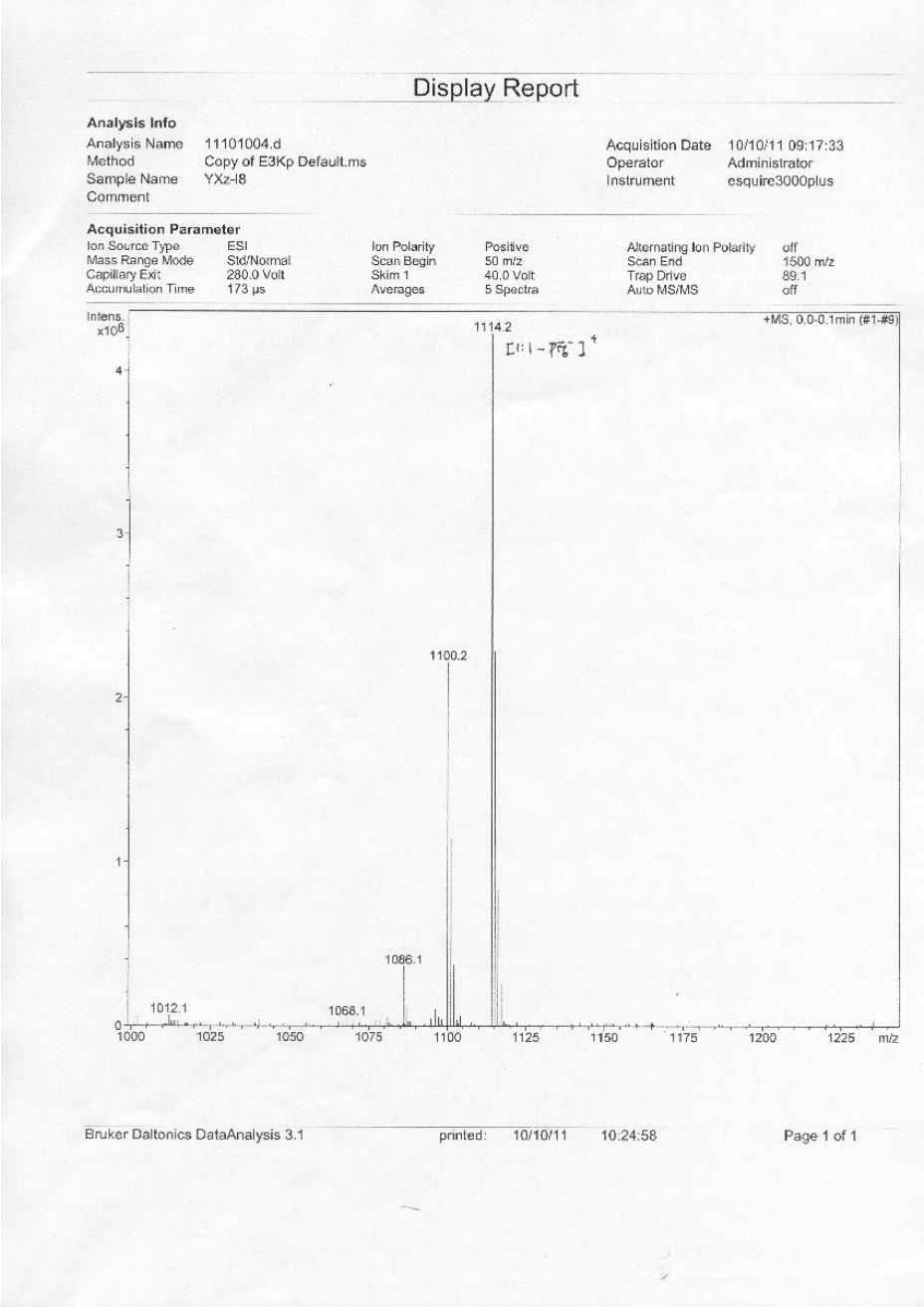

Fig. S2. The positive electrospray ionization mass spectrum of an equimolar mixture of **2** and **4** in acetone. Mass fragments at *m/z* 1114.2 for $[\mathbf{2}\supset\mathbf{4} - PF_6]^+$ and *m/z* 484.8 for $[\mathbf{2}\supset\mathbf{4} - 2PF_6]^{2+}$ confirmed the 1:1 complexation stoichiometry between **2** and **4**.

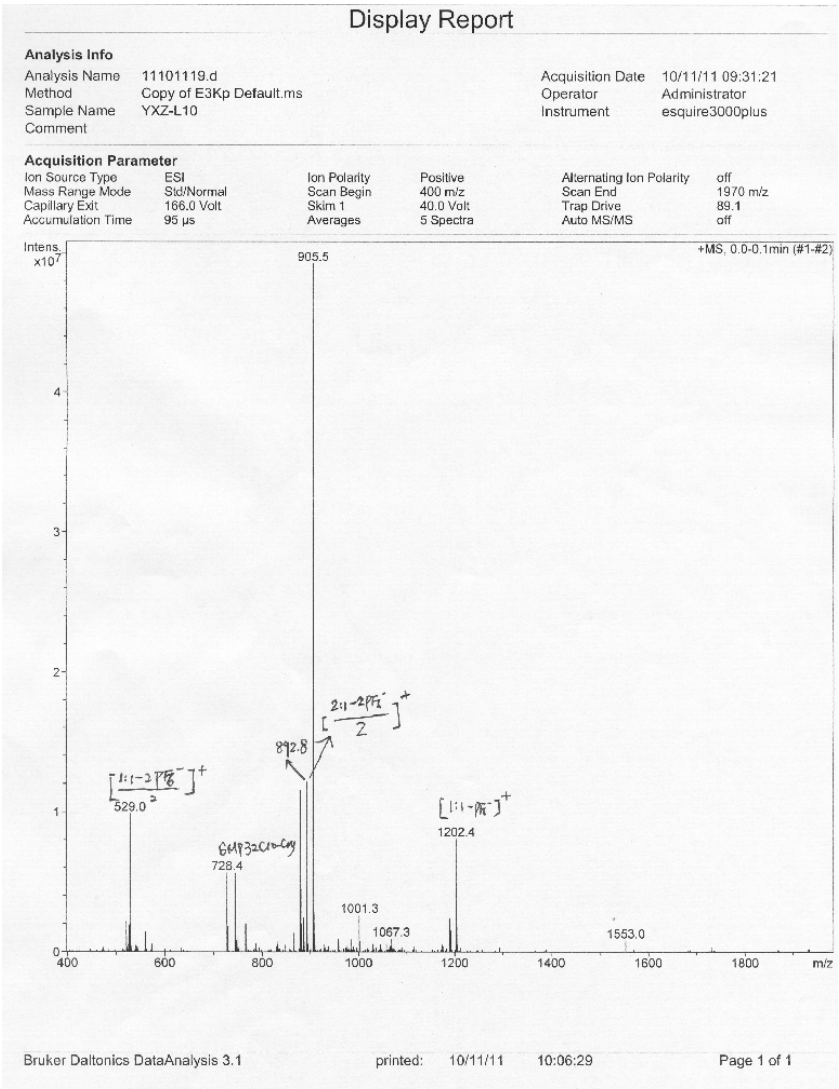

Fig. S3. The positive electrospray ionization mass spectrum of a mixture of **3** and **4** in acetone. A mass fragment at *m/z* 892.8 for $[\mathbf{3}_2\supset\mathbf{4} - 2PF_6]^{2+}$ comfirmed the 2:1 complexation stoichiometry between **3** and **4**. Assignment of other main peaks: *m/z* 1202.4 for $[\mathbf{3}\supset\mathbf{4} - PF_6]^{+}$ and *m/z* 529.0 for $[\mathbf{3}\supset\mathbf{4} - 2PF_6]^{2+}$.

4. Determination of association constant of ***2⊃4***

The association constant of complex **2⊃4** was determined by probing the charge-transfer band of the complexes by UV-vis spectroscopy and employing a titration method. Progressive addition of an acetone solution with high guest **4** concentration and low host **2** concentration to an acetone solution with the same concentration of host **2** resulted in an increase of the intensity of the charge-transfer band of the complex. Treatment of the collected absorbance data at λ = 380 nm with a non-linear curve-fitting program afforded the corresponding association constants (K_a): $(1.43 \pm 0.06) \times 10^3$ M^{-1} for **2⊃4**.

The non-linear curve-fitting was based on the equation:

$$A = (A_\infty/[H]_0)\ (0.5[G]_0 + 0.5([H]_0+1/K_a)-(0.5\ ([G]_0^2+(2[G]_0(1/K_a - [H]_0)) + (1/K_a + [H]_0)^2)^{0.5})) \qquad \text{(Eq. S1)}$$

Where A is the absorption intensity of the charge-transfer band (λ = 380 nm) at $[G]_0$, A_∞ is the absorption intensity of the charge-transfer band (λ = 380 nm) when the host is completely complexed, $[H]_0$ is the fixed initial concentration of the host, and $[G]_0$ is the initial concentration of the guest.

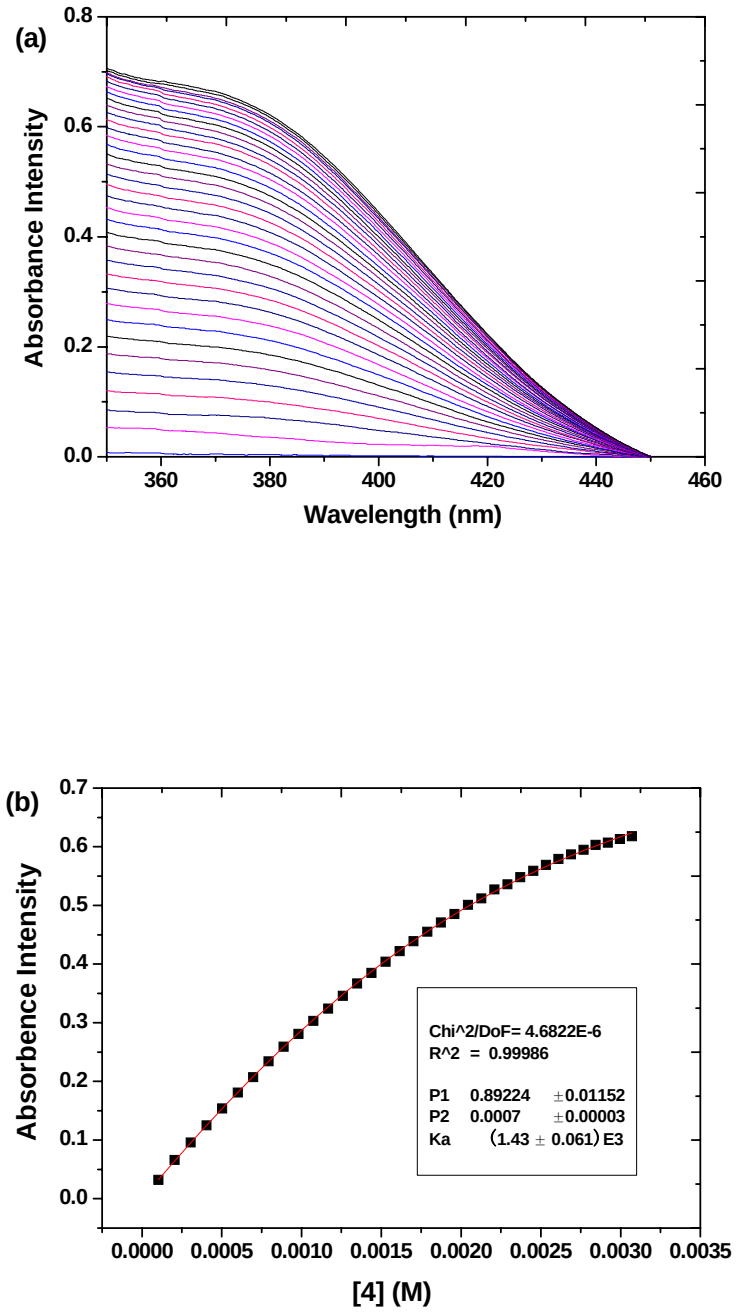

Fig. S4. (a) The absorption spectral changes of **2** upon addition of **4** and (b) the absorbance intensity changes upon addition of **4**. The red solid line was obtained from the non-linear curve-fitting using Eq. S1.

5. Determination of average association constant of $\mathbf{3}_2\supset\mathbf{4}$

The average association constant of complexes $\mathbf{3}_2\supset\mathbf{4}$ was determined by probing the charge-transfer band of the complexes by UV-vis spectroscopy and employing a titration method. Progressive addition of an acetone solution with high cryptand **3** concentration and low guest **4** concentration to an acetone solution with the same concentration of guest **4** resulted in an increase of the intensity of the charge-transfer band of the complex.

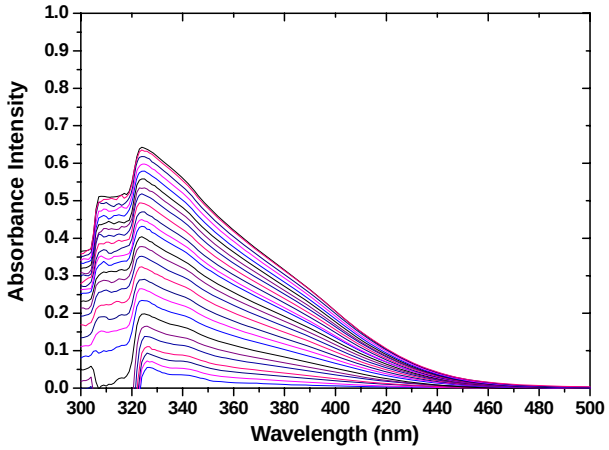

Fig. S5. The absorption spectral changes of **4** upon addition of **3**.

Treatment of the collected absorbance data at λ = 350 nm by Benesi-Hildebrand method[S6] and Scatchard plot method.[S7] The ΔA_∞ can be determined by extrapolation of a plot of $1/\Delta A$ vs. $1/[\mathbf{3}]_0$ by the Benesi-Hildebrand method. The association constant K_{av} can be calculated from the intercept and the slope of the Scatchard plot.

$\Delta A = A - A_0$

$\Delta A_\infty = A_\infty - A_0$

$p = \Delta A / \Delta A_\infty$

$[\mathbf{3}] = [\mathbf{3}]_0 - [\mathbf{3}]_c = [G]_0 - 2p[\mathbf{4}]_0$

A_0 is the initial absorbance of **4**, A_∞ is the absorbance of the fully complexed species, ΔA_∞ is the difference in the absorbance of uncomplexed and fully complexed species, p is the fraction of guest **4** units bound, [**3**] is the concentration of uncomplexed **3**, $[\mathbf{3}]_0$ is the initial concentration of **3**, $[\mathbf{3}]_c$ is the concentration of complexed **3**, and $[\mathbf{4}]_0$ is the initial concentration of **4**.

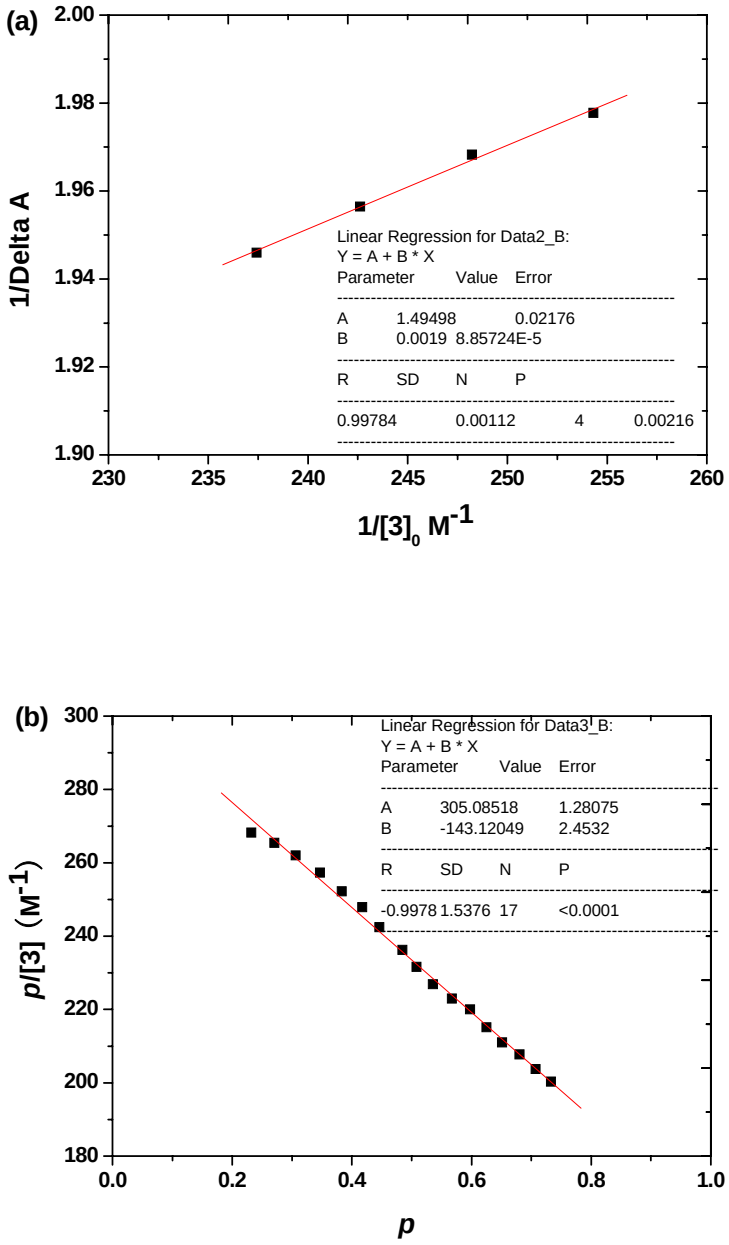

Fig. S6. (a) Benesi-Hildebrand plot for the complexation of host **3** with guest **4**. ΔA_{∞} = 1/1.49498 = 0.6689 according to the intercept of the plot. (b) Scatchard plot for the complexation of host **3** with guest **4**. *p* = fraction of guest **4** units bound. The linear nature of this plot demonstrated that the complexation between host **3** and guest **4** is statistical. K_1 = [**3**⊃**4**]/{[**3**][**4**]} and K_2 = [**3**$_2$⊃**4**]/{[**3**⊃**4**][**4**]}. K_{av} = (K_1 + K_2)/2. The value of K_{av} is equal to the *y*-intercept and the absolute slope of the best fit line. K_{av} = (305 + 143) / 2 = 224 M^{-1}. Since K_1/K_2 = 4:1 for statistical systems, K_1 and K_2 were calculated to be 360 M^{-1} and 90 M^{-1}, respectively.

*6. Partial 2D COSY NMR spectrum of an equimolar solution of **2** and **4***

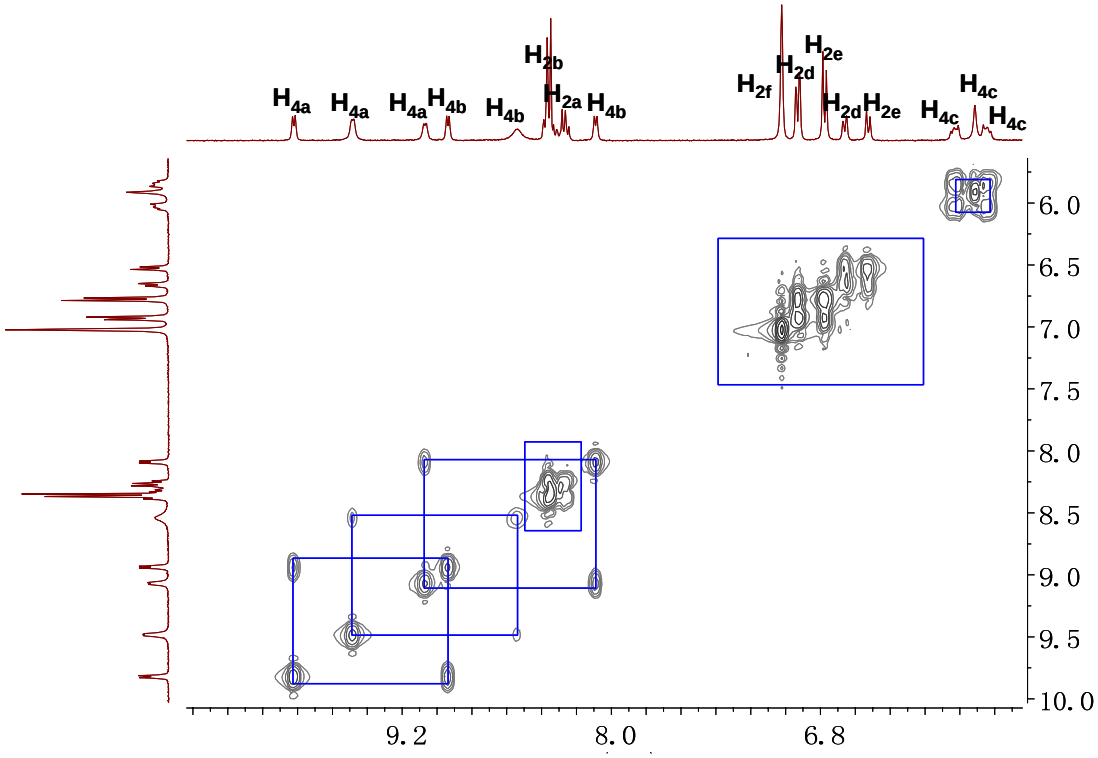

Fig. S7. Partial 2D COSY NMR (400 MHz, acetone-d_6, 293 K) spectrum of an equimolar solution of **2** and **4** at a concentration of 10.0 mM.

7. X-ray crystal data for ***2***$_2$⊃***4***

Crystallographic data: block, yellow, 0.46 × 0.36 × 0.34 mm^3, $C_{44}H_{51}F_6N_3O_{14}P$, *FW* 990.85, triclinic, space group *P*−1, *a* = 10.7671(5), *b* = 14.3961(6), *c* = 14.9463(6) Å, *α* = 95.617(4)°, *β* = 91.069(4)°, *γ* = 97.164(4)°, *V* = 2286.49(17) Å^3, *Z* = 2, D_c = 1.439 g cm^{-3}, *T* = 293 (2) K, *μ* = 1.367 mm^{-1}, 25194 measured reflections, 8097 independent reflections, 639 parameters, 0 restraints, *F*(000) = 1034, *R*(int) = 0.0413, R_1 = 0.0973, wR_1 = 0.2013 (all data), R_2 = 0.0746, wR_2 = 0.1823 [$I > 2\sigma(I)$], max. residual density 1.293 e•Å^{-3}, and goodness-of-fit (F^2) = 1.040. CCDC 849131.

8. X-ray crystal data for ***3***$_2$⊃***4***

Crystallographic data: block, yellow, 0.24 × 0.23 × 0.20 mm^3, $C_{40}H_{46}F_6N_2O_{12}P$, *FW* 2191.95, triclinic, space group *P*−1, *a* = 11.0344(3), *b* = 18.43766(4), *c* = 22.9640(5) Å, *α* = 99.5446(17)°, *β* = 104.4477(18)°, *γ* = 108.5331(19)°, *V* = 5257.53(19) Å^3, *Z* = 2, D_c = 1.385 g cm^{-3}, *T* = 293 (2) K, *μ* = 1.280 mm^{-1}, 76330 measured reflections,18669 independent reflections, 1378 parameters, 0 restraints, *F*(000) = 2300, *R*(int) = 0.0472, R_1 = 0.01157, wR_1 = 0.2740 (all data), R_2 = 0.0921, wR_2 = 0.2486 [$I > 2\sigma(I)$], max. residual density 1.197 e•Å^{-3}, and goodness-of-fit (F^2) = 1.040. CCDC 867881.

9. Design of cryptands ***2*** *and* ***3***

The design of cryptands **2** and **3** was reported previously.[S1,S2]

10. Reasons for different stoichiometries of the complexation between ***2*** *and* ***4*** *in solution and in the solid state*

The complexation between **2** and **4** has a 1:1 stoichiometry in solution and a 2:1 stoichiometry in the solid state. This interesting phenomenon was also observed in previous studies.[S2,S9] It appears that the formation of the 2:1 complex in the solid state is to maximize H-bonding between the host and the guest;[S2] it produces eight hydrogen bonds between six hydrogen atoms of guest **4** and six oxygen atoms of two cryptand **2** hosts (Fig. 4). In solution, presumably some of these acidic pyridinium and bridge ethane hydrogen atoms can interact with solvent molecules and the host and guest molecules have more room to move freely, so the complex between **2** and **4** has a 1:1 stoichiometry.[S2]

*11. Influence of the addition of KPF_6 on the complexation between **3** and **4***

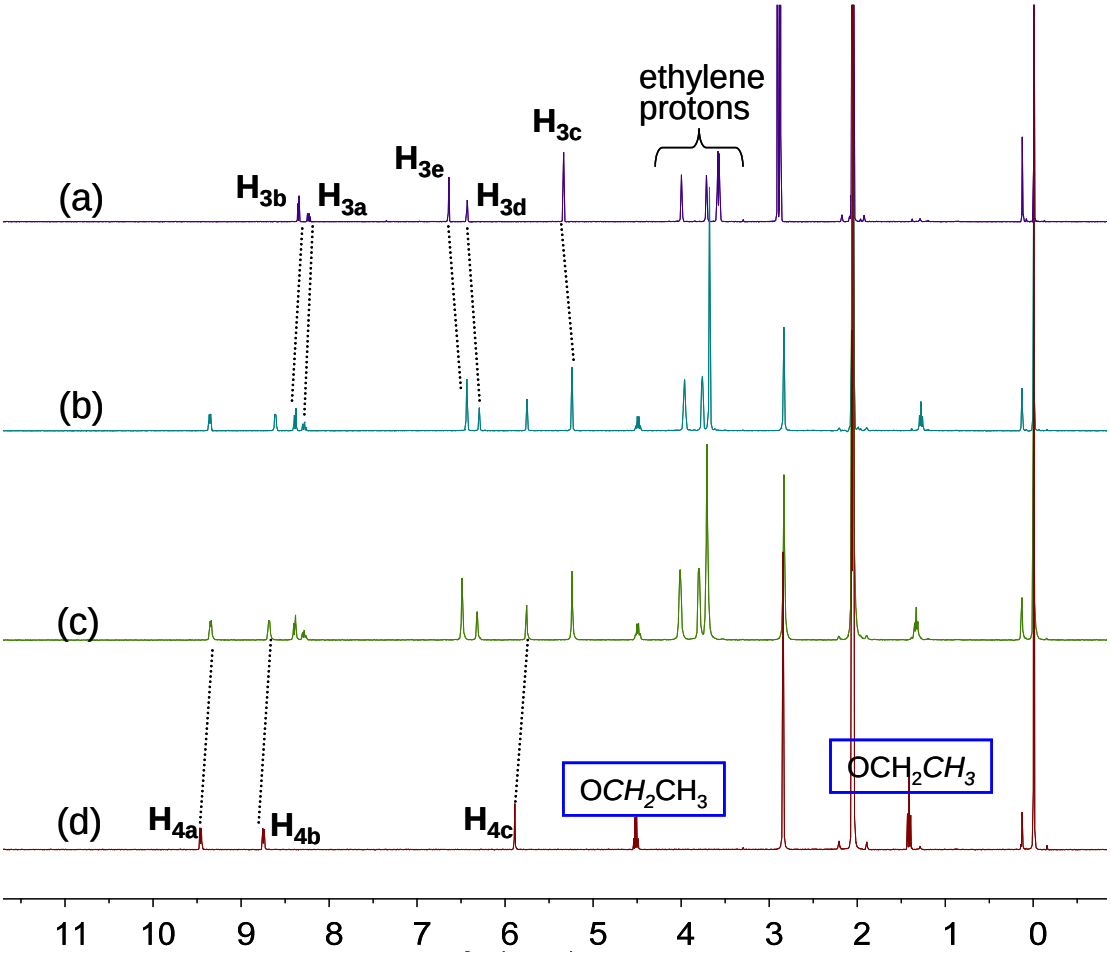

Fig. S8. Partial ^{1}H NMR (400 MHz, acetone-d_6, 293 K) spectra: (a) 4.00 mM **3**; (b) 4.00 mM **3** + 2.00 mM **4**; (c) after addition 2.00 equiv of KPF_6 to b; (d) 2.00 mM **4**.

The chemical shifts of the protons on **3** and **4** did not have obvious changes after the addition of 2.00 equiv of KPF_6 (spectra b and c in Fig. S8), indicating that the addition of potassium cation can not switch off the complexation between **3** and **4** easily.

References:

S1. H. W. Gibson, H. Wang, C. Slebodnick, J. Merola, W. S. Kassel and A. L. Rheingold, *J. Org. Chem.*, 2007, **72**, 3381.

S2. F. Huang, K. A. Switek, L. N. Zakharov, F. R. Fronczek, C. Slebodnick, M. Lam, J. A. Golen, W. S. Bryant, P. E. Mason, A. L. Rheingold, M. Ashraf-Khorassani and H. W. Gibson, *J. Org. Chem.*, 2005, **70**, 3231.

S3. S. J. Loeb and J. A. Wisner, *Angew. Chem., Int. Ed.*, 1998, **37**, 2838.

S4. G. M. Sheldrick, *SHELXS-97*, *Program for solution of crystal structures*, University of Göttingen, Germany, 1990.

S5. G. M. Sheldrick, *SHELXS-97*, *Program for refinement of crystal structures*, University of Göttingen, Germany, 1997.

S6. H. A. Benesi and J. H. Hildebrand, *J. Am. Chem. Soc.,* 1949, **71**, 2703.

S7. (a) A. G. Marshall, *Biophysical Chemistry*; J. Wiley and Sons: New York, 1978; pp 70–77. (b) D. M. Freifelder, *Physical Biochemistry*; W. H. Freeman and Co. New York, 1982; pp 659–660. (c) K. A. Connors, *Binding Constants*; J. Wiley and Sons: New York, 1987; pp 78–86.

S8. W. S. Bryant, J. W. Jones, P. E. Mason, I. Guzei, A. L. Rheingold, F. R. Fronczek, D. S. Nagvekar and H. W. Gibson, *Org. Lett.*, 1999, **1**, 1001.

S9. F. Huang, H. W. Gibson, W. S. Bryant, D. S. Nagvekar and F. R. Fronczek, *J. Am. Chem. Soc.,* 2003, **125**, 9367.